**Distribution Agreement**

In presenting this thesis as a partial fulfillment of the requirements for a degree from Emory University, I hereby grant to Emory University and its agents the non-exclusive license to archive, make accessible, and display my thesis in whole or in part in all forms of media, now or hereafter know, including display on the World Wide Web. I understand that I may select some access restrictions as part of the online submission of this thesis. I retain all ownership rights to the copyright of the thesis. I also retain the right to use in future works (such as articles or books) all or part of this thesis.

Grace Zhou April 10, 2023

# YB-1 Promotes PLXND1 mRNA Translation to Mediate Tumor Migration in Sonic Hedgehog Medulloblastoma

by

Grace Zhou

Anna Kenney

Adviser

Neuroscience and Behavioral Biology

Anna Kenney

Adviser

Kristen Frenzel

Committee Member

Sumin Kang

Committee Member

2023

# YB-1 Promotes PLXND1 mRNA Translation to Mediate Tumor Migration in Sonic Hedgehog Medulloblastoma

By

Grace Zhou

Anna Kenney

Adviser

An abstract of

a thesis submitted to the Faculty of Emory College of Arts and Sciences

of Emory University in partial fulfillment

of the requirements of the degree of

Bachelor of Sciences with Honors

Neuroscience and Behavioral Biology

2023

Abstract

YB-1 Promotes PLXND1 mRNA Translation to Mediate Tumor Migration in Sonic Hedgehog Medulloblastoma

By Grace Zhou

Medulloblastoma (MB) is one of the most common malignant pediatric brain cancers. Tumor metastasis is associated with higher risk, and recurrence is often fatal. The current treatment regimen is highly toxic and often results in severe complications, including cognitive and endocrine sequelae. In this study, we propose a novel role of Y-box binding protein-1 (YB-1) in positively modulating PlexinD1 (PLXND1) translation and its effect on MB migration. We show that PLXND1, its ligand Semaphorin 3E, and its binding partner Neuropilin-1 promote migration in Sonic Hedgehog (SHH) MB. Further, we explore the therapeutic potential of a PLXND1 binding peptide, which has previously been used in pancreatic adenocarcinoma research. Our findings indicate that the PLXND1 binding peptide reduces cell growth and epithelial-to-mesenchymal transition in SHH MB cells, suggesting that targeting PLXND1 may impair tumor growth and migration in SHH MB. Our study offers a potential avenue for therapeutic inhibition of SHH MB through targeting PLXND1.

# YB-1 Promotes PLXND1 mRNA Translation to Mediate Tumor Migration in Sonic Hedgehog Medulloblastoma

By

Grace Zhou

Anna Kenney

Adviser

A thesis submitted to the Faculty of Emory College of Arts and Sciences

of Emory University in partial fulfillment

of the requirements of the degree of

Bachelor of Sciences with Honors

Neuroscience and Behavioral Biology

2023

Acknowledgements

My gratitude to Leon McSwain, my direct mentor, for his guidance throughout the completion of my thesis and teaching during my undergraduate research career. I am grateful for his encouragement and humor while preparing me for the challenges of scientific research. I would also like to thank Dr. Kenney for providing me with the opportunity and environment to grow as a scientific thinker. My thanks goes out to my committee members Dr. Frenzel for her wisdom as my Neuroscience and Behavioral Biology advisor and research mentor and to Dr. Kang for her eagerness to lend me her expertise during the completion of my thesis. I am forever grateful to Dr. Brian Olsen, my former committee member who provided me with valuable insights before his unfortunate passing. I would like to thank my Kenney lab members who have provided me with support and assistance during the research process. Lastly, I owe my deepest thanks to my parents, who have provided me with unconditional love and support throughout my life. I am grateful for all the sacrifices they have made that make it possible for me to pursue my dreams.

## Table of Contents



**Figures**

# Introduction

## Medulloblastoma and treatment outcomes

Medulloblastoma (**MB**) is the most common malignant childhood brain cancer, comprising 10–20% of all pediatric brain tumors[1,2]. Arising in the posterior fossa, MB is classified into four distinct molecular subgroups: wingless (**WNT**), sonic hedgehog (**SHH**), Group 3, and Group 4.[1] SHH MB, originating from cerebellar granule neural precursor cells (**CGNPs**) of the cerebellum, is characterized by perturbations in SHH signaling, a key embryonic developmental signaling axis.[3–5] Alterations in the Hedgehog pathway involving the SHH –| Ptch1 –| Smo → Gli signaling axis characterize SHH MB.[3,4] Mutations that lower Ptch1 expression or constitutively express Smo result in higher Gli nuclear translocation, driving tumor progression.

SHH MB accounts for 30% of all MBs and predominantly affects young children and older adolescents.[1] Prognosis depends upon tumor histology, with a 10-year survival rate ranging from 84% to 34%.[1] The typical treatment regimen includes tumor resection, radiation therapy, and chemotherapy; however, treatments pose high risk of morbidity in pediatric patients, often accompanied with cognitive and endocrine sequelae including hearing loss, pituitary damage, and secondary malignancies.[2] MB recurrence is observed in 30% of patients and is often fatal.[5] In patients with MB recurrence previously treated with cranial-spinal irradiation, the five-year survival rate is 10%.[5] The fatality of MB recurrence and stagnation of new treatment developments, partially due to off-target toxicity, identifies a need for further research investigating novel subgroup and signaling-specific targets in MB.

## The roles of Y-box binding protein 1 (YB-1)

Our group has previously identified Y-box binding protein 1 (**YB-1**) as a driver of SHH MB oncogenesis.[6] The roles of YB-1 are multifaceted–as both a DNA and RNA-binding protein, YB-1 regulates pathways involved in cell cycle progression, DNA repair, and cellular stress responses.[7] In cancer, YB-1 drives tumor proliferation, invasion, metastasis, and chemotherapy resistance.[7,8] Previously, our lab has shown YB-1 requirement for CGNP and MB proliferation, elevation across all MB subgroups, and its involvement as a downstream target of SHH signaling.[6] Current findings show robust levels of YB-1 protein in all MB subgroups and elucidates a potential signaling axis in which YB-1 post-transcriptionally regulates and promotes Plexin-D1 (**PLXND1**) translation to drive migration and invasion in SHH MB (**Figure 1)**.

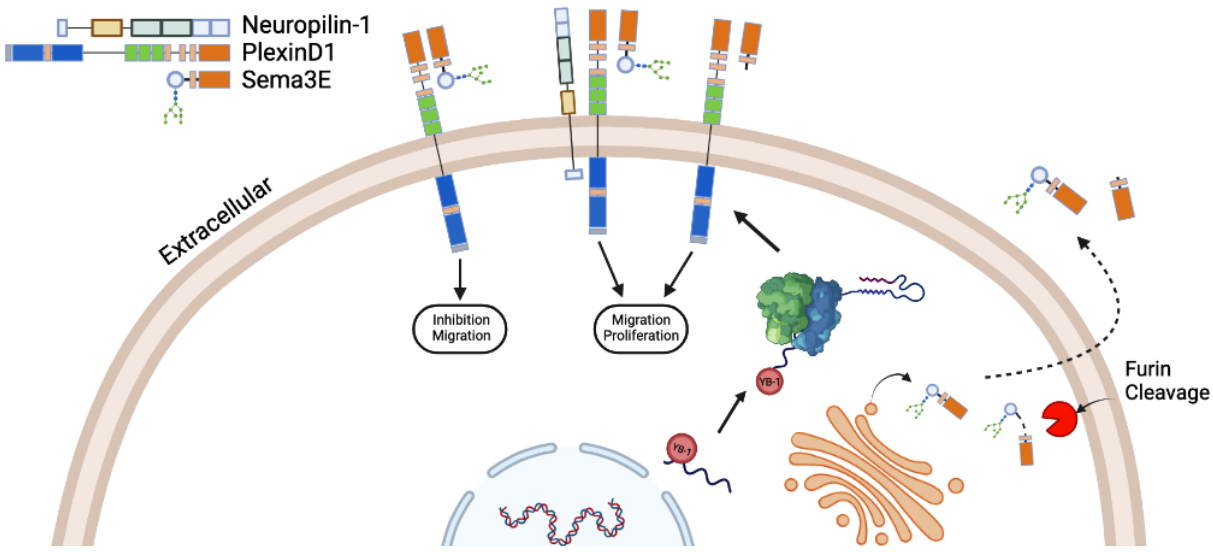


**Figure 1: YB1 post-transcriptionally drives PLXND1 expression.** When full-length SEMA3E binds PLXND1 in isolation, the result is typically a repulsive or migration inhibitory effect. Binding to a PLXND1/NRP1 complex can result in a migratory phenotype. SEMA3E can

be cleaved by Furin to produce a 62kDa and 25kDa fragment that can also be glycosylated in the golgi body prior to secretion. Binding of cleaved SEMA3E to PlexinD1 in isolation is sufficient to induce migration.

**Developmental role of Plexins and Semaphorins**

Plexins, a class of transmembrane proteins, are cell surface receptors to semaphorins, a large family of glycoproteins that can be secreted or membrane-bound.[9,10] As axonal guidance proteins, plexin/semaphorin signaling drives central nervous system development.[11] In adult tissues, PLXND1 expression is low and limited to select fibroblasts and macrophages.[12] However, elevated PLXND1 expression occurs in several tumors and the tumor vasculature[12]. Current lab data of YB-1 RNA binding protein immunoprecipitation sequencing shows enrichment of PLXND1 transcripts bound to YB-1 protein, leading our lab to investigate PLXND1 as a potential mediator of YB-1 oncogenic function. Semaphorin3E (**SEMA3E**) canonically binds to PLXND1, and during neuronal development, their signaling is implicated in guiding axonal descent, promoting schwann cell proliferation and migration, stimulating migration of cranial neural crest cells, and controlling laminar development in the corpus callosum.[13–16] On the contrary, PLXND1/SEMA3E signaling has also been shown to inhibit neuronal migration, specifically in Cajal-Retzius cells in the cerebral cortex and in neurons of newborn olfactory bulbs.[17,18] Thus, PLXND1/SEMA3E signaling exhibits context-dependent functions, which either promotes or inhibits axonal growth and cell migration. While Plexin-B2 is implicated in driving cerebellar development, the developmental role for PLXND1 remains unknown.[19]

**PLXND1, SEMA3E, and Nrp1 binding interactions and signaling**

Before Plexins were widely accepted as the canonical binding partners of semaphorins, neuropilins were considered the typical binding moieties of class three semaphorins.[20] Previously, Nrp1/Semaphorin signaling was understood to control repulsion in neuronal migration and axonal guidance, with growing evidence suggesting the same signaling molecules could also elicit axonal attraction.[20] One novel study on class three semaphorins reported that the cytoplasmic end of NRPs appeared too short to independently signal through semaphorins. PLXND1 was then hypothesized to be a coreceptor involved in mediating semaphorin signal transduction.[10] Building upon this observation, another study demonstrated that Neuropilin-1 (**Nrp1**) can bind class three semaphorins. This study showed that on corticofugal and striatonigral neurons, which expressed PLXND1 but not Nrp1, SEMA3E repelled axonal projections. In mammillary neurons that expressed both PLXND1 and Nrp1, however, SEMA3E attracted axonal projections.[13] Thus, PLXND1 and Nrp1 are both implicated in SEMA3E signaling, with opposing effects on cell migration. While the exact mechanisms by which PLXND1 exerts inhibitory or migratory effects are unclear, there is evidence that when full length PLXND1 binds SEMA3E, the resulting effect is typically inhibitory, while SEMA3E binding to PLXND1/Nrp1 complex results in a migratory phenotype (**Figure 1**).[21] Further, SEMA3E undergoes furin-mediated cleavage into p61 and p26 isoforms, which have differential effects upon migratory activity among cancers.[22]

**Plexin-D1 and Semaphorin 3E Oncogenesis**

PLXND1/SEMA3E dysregulation occurs in several cancers and has been shown to drive tumor angiogenesis and metastasis.[21] In gastric cancer, pancreatic adenocarcinoma, and colon carcinoma, PLXND1/SEMA3E signaling and expression were involved in cancer cell proliferation, metastasis, and invasion.[23–25] Studies have also linked PLXND1/SEMA3E signaling

to epithelial to mesenchymal transition (EMT), a hallmark of tumor expansion, in colorectal and ovarian cancers.[22,26,27] In breast cancer, SEMA3E expression has been shown to suppress apoptosis and increase cancer cell survival.[28] Given the lack of existing research investigating PLXND1/SEMA3E signaling in MB, we seek to characterize a role for PLXND1 and SEMA3E interactions to further understand metastatic signaling in SHH MB.

**Preliminary Data**

Previous data from our group has established that YB-1 post-transcriptionally regulates and promotes PLXND1 expression in SHH MB. Specifically, RNA binding protein immunoprecipitation sequencing of YB-1 protein shows significant PLXND1 mRNA enrichment, leading to our interest in PLXND1. Gene expression analysis from a patient microarray dataset consisting of 763 MB patient samples revealed significantly enriched PLXND1 transcripts in the SHH subgroup relative to all other MB subgroups (GEO accession GSE85217). Our group has also found significantly increased PLXND1 protein expression in primary mouse model SHH MB tumors compared to matched normal cerebellar tissue. Furthermore, we have shown consistently decreased PLXND1 protein expression upon YB-1 shRNA knockdown in multiple SHH MB cell lines and a reduction in cell migration upon PLXND1 knockdown. Given our preliminary findings, we aim to further validate the YB-1/PLXND1 signaling axis and investigate the role of PLXND1 binding proteins in SHH MB migration.

**Hypothesis and Aims**

Despite research on PLXND1-SEMA3E signaling in other cancer models, there are currently no studies on this signal axis in MB. Current lab data show PLXND1 protein enrichment

in SHH MB and suggest that YB-1 post-transcriptionally regulates PLXND1 expression to mediate cell migration. As a continuation of the ongoing project, this thesis will investigate the SEMA3E signaling axis and receptor dependency for PLXND1 signaling, proliferation, and migration. We will separate our investigation into two aims:

**Aim 1:** Characterize the YB-1 → PLXND1 signaling axis (**Figure 2**)

**Subaim a:** Determine the requirement for PLXND1 in YB-1 mediated cell migration

**Aim 2:** Characterize PLXND1 binding partners and ligands (**Figure 2**)

**Subaim a:** Characterize the expression, glycosylation, and secretion of SEMA3E

**Subaim b:** Determine the requirement for SEMA3E and Nrp1 for cell migration

**We hypothesize that 1) PLXND1 is required for YB-1-mediated cell migration, and 2) SEMA3E signals through PLXND1 and/or Nrp1 to mediate a pro-migratory phenotype in SHH MB.**

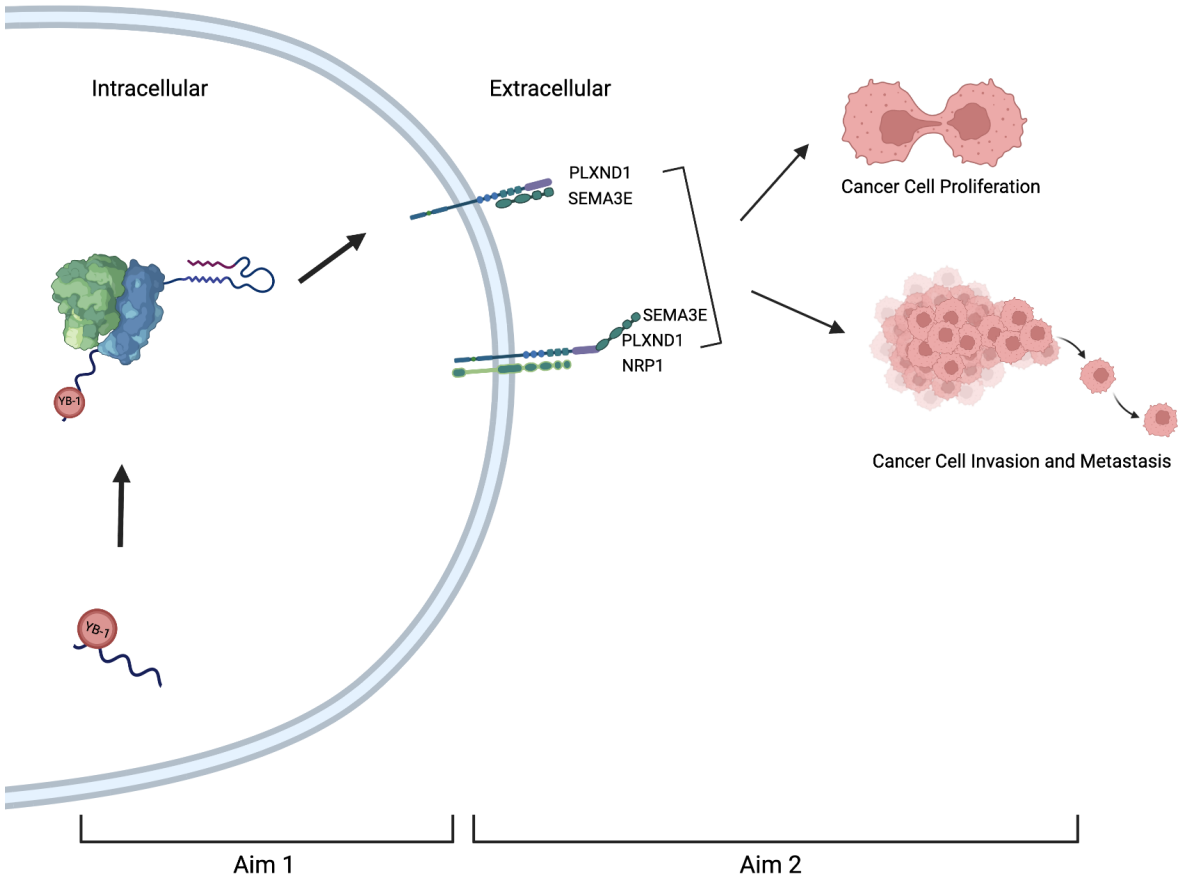
Intracellular
Extracellular
YB-1
YB-1
PLXND1
SEMA3E
SEMA3E
PLXND1
NRP1
Cancer Cell Proliferation
Cancer Cell Invasion and Metastasis
Aim 1
Aim 2

**Figure 2: Depiction of specific aims.** Specific Aim 1: characterization of YB-1 → PLXND1 signaling axis. Specific Aim 2: characterization of PLXND1 binding partners and ligands and their requirement for cancer cell migration.

## Materials and Methods:

### Cell Culture

Human SHH MB cell lines UW228 gifted by Dr. Tobey MacDonald and ONS-76 from American Type Culture Collection and mouse SHH MB cell line PZp53MED (PZP) gifted by Dr. Matthew Scott were cultured in Dulbecco's Modified Eagle Medium/Nutrient Mixture F-12[29]. Media contained 10% fetal bovine serum (FBS) supplement and 1% penicillin-streptomycin. Cells were stored in a humidified incubator with 5% CO2 at 37˚C.

### shRNA Generation and Lentiviral Transduction

Stable knockdown cell lines (shPLXND1_50, shPLXND1_52, shSEMA3E_34, shSEMA3E_35, shNRP1_17, shNRP1_27, and non-targeting control shSCR) were generated using lentiviral-mediated delivery of shRNA constructs followed by puromycin selection. shRNA-carrying lentivirus was generated using HEK 293T transfection.

### Wound Healing Scratch Assay

300,000 cells were seeded into 6-well plates and cultured in 2.5% FBS media overnight to confluence. A 1000 $u$L pipette tip was used to vertically scratch the cell monolayer. Images of the scratched area were obtained at the time of initial scratch and at 24 and 48 hours post-scratch. Cell migration was measured using ImageJ software and evaluated by wound area.

**Proliferation Assay**

75,000 cells were plated for all conditions. Cells were counted four days after plating.

**Immunofluorescence**

Cells were fixed using 10% paraformaldehyde, washed with phosphate buffered saline, blocked with 5% bovine serum albumin and 3% normal goat serum. Cells were stained with the following primary antibodies (anti-PLXND1, anti-SEMA3E, anti-NRP1, anti-Caspase-3, anti-cPARP, anti-HIF1A). Binding of the antibodies were detected using 488 and 594 anti-goat secondary and co-stained with DAPI.

**Western Blotting**

Cells were lysed in RIPA buffer containing phosphatase and protease inhibitors (Thermo Scientific). Protein samples (15ug) were denatured and separated on 8-12% SDS-PAGE gels and transferred to immobilon-P PVDF membranes (Millipore). After blocking with 5% milk in tris-buffered saline with 0.1% tween (TBST), the membranes were incubated overnight in primary antibodies. The following primary antibodies were used: PLXND1 (NBP1-33634;NOV), SEMA3E (AF3239; RnD), NRP1 (AF566; RnD), β-Tubulin (sc-177829; SCBT), N-Cadherin (D4R1H; CST), E-Cadherin (24E10; CST), Slug (C19G7; CST), Snail (C15D3; CST), and Claudin-1 (D5H1D; CST). After incubating with secondary antibodies, blots were developed using pierce ECL Western Blotting Substrate or SuperSignal West Pico PLUS Chemiluminescent

Substrate (Thermo Scientific). (NOV: Novus Biologicals, SCBT: Santa Cruz Biotechnology, CST: Cell Signaling Technology).

### Inhibitor Time Course

25 uM of proteasome inhibitor MG132, 7 ug of transcription inhibitor Actinomycin D, and 10.5 uL of dimethyl sulfoxide as a negative control were added to confluent cells and incubated for six hours. Cells were lysed in RIPA buffer and protein samples were prepared as detailed above.

### PlexinD1 Binding Peptide Incubation

PLXND1 binding peptide and a scrambled control peptide were introduced into cell culture media at 50uM for 2 hours and 100 uM for 3 hours. Cells were harvested for protein lysate immediately at the end of the time course.

## Results

### YB-1 regulates PLXND1 mRNA Translation

We first confirmed previous findings from our group, showing elevated PLXND1 expression in primary mouse medulloblastoma cells (**MB**) compared to non-tumor cerebellar tissue (**CB**) (**Figure 3a**). Previous data has shown a significant decrease in PLXND1 protein upon shRNA-mediated knockdown of YB-1 in PZP and ONS-76 SHH MB cell lines and in a primary MB mouse tumor model (**MBC**) (**Figure 3b,c**). However, PLXND1 RNA levels did not change after YB-1 knockdown, suggesting that YB-1 has a post-transcriptional regulatory role in PLXND1 expression (**Figure 3d**). We hypothesized the YB-1 regulated PLXND1 mRNA translation. In order to confirm our hypothesis, we needed to eliminate potential confounding

explanations for the change in PLXND1 protein levels, including differences in transcription turnover rate and/or in protein degradation rates. Thus, we introduced proteasome inhibitor MG132 and transcription inhibitor actinomycin D (ActD) to inhibit protein degradation and transcription, respectively, in UW228 cell lines.[30,31] We used ubiquitin (Ub) and γH2AX as positive controls for MG132 and ActD, respectively, and DMSO as the negative control for both inhibitor conditions. We used β-tubulin as the loading control, and the shSCR cell line served as a negative control for the shYB-1 cell line. By inhibiting both transcription and protein degradation, we allowed only translation to occur, ensuring that any changes in PLXND1 protein levels are attributed only to YB-1 post-transcriptional modification. The single inhibitor conditions validated the proper activity of the inhibitors, with Ub levels increasing in the MG132 condition and γH2AX levels increasing after ActD introduction (**Figure 3d**). Consistent with our hypothesis, we observed a decrease in PLXND1 protein levels following YB-1 knockdown in the combination

translation and proteasome inhibitor condition (**Figure 3d**). Our data suggest that YB-1 positively regulates PLXND1 mRNA translation.

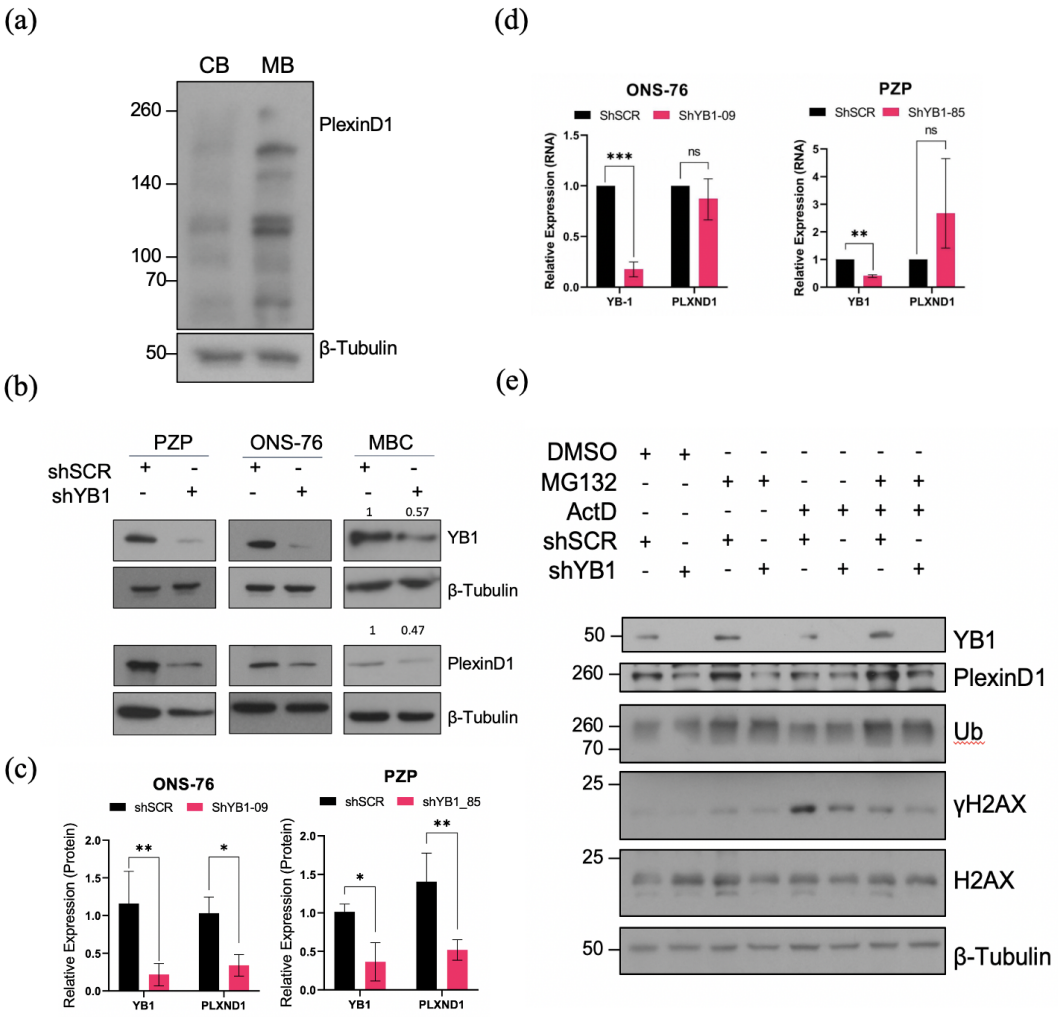

**Figure 3: YB-1 regulates PLXND1 mRNA Translation. (A)** Western blotting showing increased PLXND1 expression in primary mice medulloblastoma cells (MB) relative to non-tumor cerebellar tissue (CB). **(B)** Western blotting showing reduced PLXND1 following YB-1 knockdown (shYB-1) in PZP, ONS-76 and MBC SHH MB cell lines. Courtesy of Victor Chen and Leon McSwain. (**C**) Western blot analysis of YB-1 and PLXND1 in ONS-76 and PZP shSCR (control) and shYB-1 constructs. Courtesy of Victor Chen and Leon McSwain. (**D**) Quantitative reverse transcription PCR (RT-qPCR) analysis demonstrating non-significant changes in PLXND1 RNA expression upon YB-1 knockdown in ONS-76 (YB-1, p=0.0026; PLXND1, p=0.3967) and PZP (YB-1, p=0.0028; PLXND1, p=0.2364). Relative expression was calculated as 2-ΔΔCt fold change, mean ± range (n=3). Paired t-test, *p≤0.05, **p≤0.01, ***p≤0.001. Courtesy of Victor Chen and Leon McSwain. (**E**) Western blotting for YB-1, PLXND1, Ub, $\gamma$H2AX, H2AX, and β-tubulin upon DMSO, MG132, ActD, and MG132 + ActD treatments in shSCR and shYB1 UW228 cell lines.

**PLXND1 depletion results in reduced tumor cell migration, proliferation, and select EMT marker shift**

In order to elucidate the role of PLXND1 in cell migration, we performed *in vitro* wound healing scratch assays using PLXND1 knockdown cells (shPLXND1_50 and shPLXND1_52) in the UW228 cell line. Consistent with our previous findings in other MB cell lines, we observed a significant reduction in wound closure upon PLXND1 knockdown compared to our non-specific shSCR control (**Figure 4a**). At 24 hours post-scratch, the shPLXND1_50 and shPLXND1_52 constructs showed an average of 34.35% and 33.81% reduction in wound closure, respectively, compared to the shSCR control. At 48 hours post-scratch, the shPLXND1_50 and shPLXND1_52 constructs showed an average of 64.36% and 61.68% reduction in wound closure, respectively,

compared to the shSCR control (**Figure 4b**). Both PLXND1 knockdown constructs showed significantly reduced ($p<0.05$) wound healing compared to the control at both time points post-scratch. These data suggest that PLXND1 promotes cell migration in SHH MB.

Further, we investigated the role of PLXND1 in cell proliferation. Four days after plating an equal number of UW228 cells, we observed a decrease in proliferation by an average of 59.17% and 39.47% among the shPLXND1_50 ($p<0.01$) and shPLXND1_52 ($p<0.5$) knockdown constructs (**Figure 4c**). These data suggest that PLXND1 may promote cellular proliferation in SHH MB.

To better understand the role of PLXND1 in cell invasion, we performed Western Blotting on UW228 cells with PLXND1 knockdown (**Figure 4d**). We probed for EMT markers including Snail, Slug, and Claudin, which increases during EMT shift–a hallmark of tumor expansion.[22,26,27] Upon PLXND1 knockdown, we observed a reduction in Slug and Claudin in both constructs, but an inconsistency in Snail among the two shPLXND1 cell lines. The inconsistency in Snail may be attributed to a transfer issue or perhaps due to an incomplete knockdown of PLXND1. Our data show a reduction in select EMT marker shifts upon PLXND1 knockdown and suggest PLXND1 plays a role in regulating tumor cell invasion.

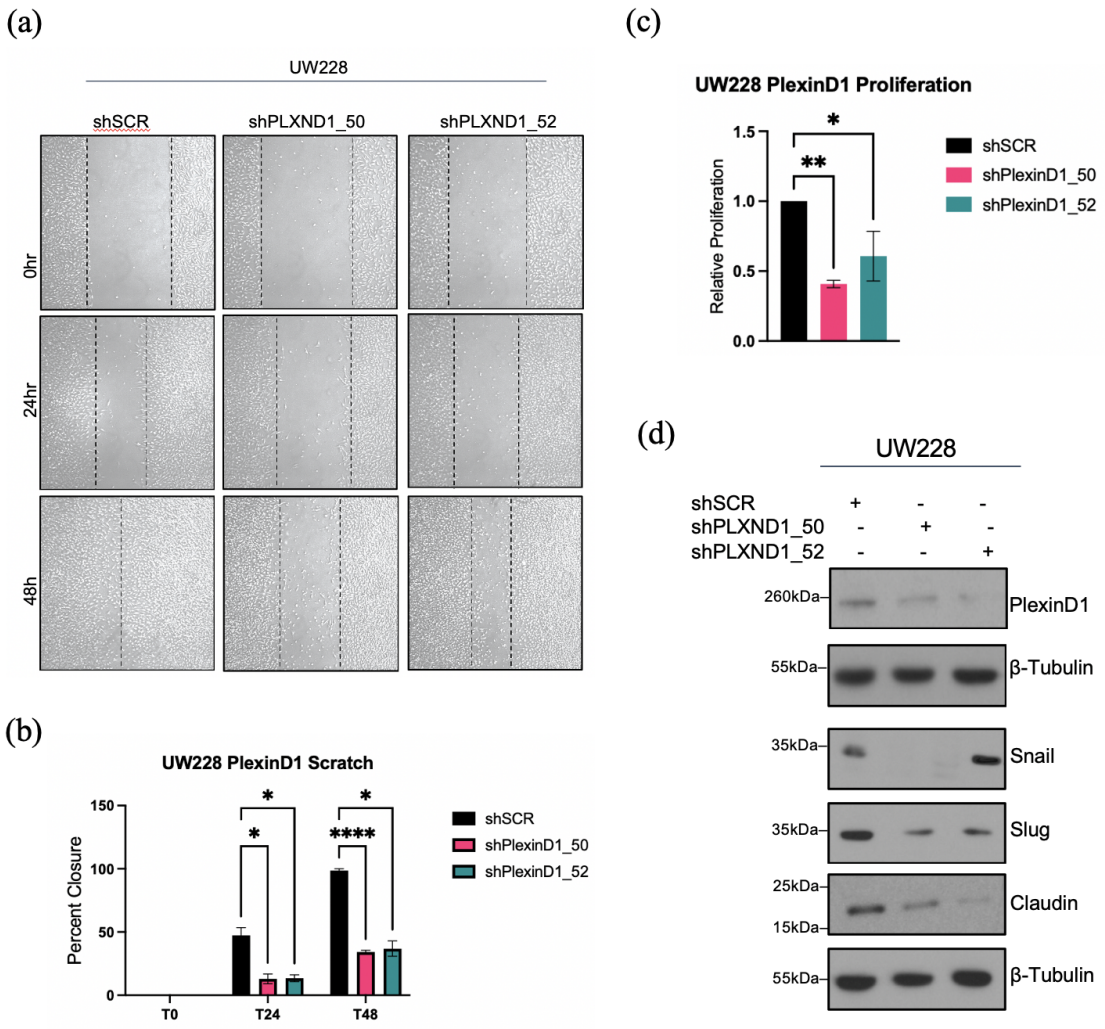


**Figure 4: PLXND1 depletion results in reduced tumor cell migration, proliferation, and select EMT marker shift. (A)** *In vitro* wound healing scratch assays in UW228 cell line with PLXND1 knockdown (shPLND1-50 and shPLXND1-52). shSCR was used as a non-specific control characteristic of wild-type UW228 cells. **(B)** Wound closure analysis showing reduced percent closure in shPLXND1-50 (T24, $p<0.05$; T48, $p<0.0001$) and shPLXND1-52(T24, $p<0.05$; T48, $p<0.01$) knockdown cell lines (n=3). **(C)** Proliferation analysis in UW228 shPLXND1_50, shPLXND1_52, and shSCR cell lines. *p<0.05, **p<0.01, ***p<0.001, ****p<0.0001, two-way

ANOVA comparing knockdown to control cell line. **(D)** Western blotting showing PLXND1 knockdown and select EMT markers.

**PLXND1 binding peptide results in reduced cell growth and EMT markers**

To investigate the translational potential of targeting PLXND1 in SHH MB, we synthesized a published PLXND1 binding peptide, which disrupts PLXND1/TGFβ binding.[12] This group showed a reduction in tumor volume in peptide-treated NSG mice injected with pancreatic ductal adenocarcinoma compared to mice treated with a scrambled control peptide.[12] We did not investigate whether TGFβ binding occurs in our models and was surprised to find that in ONS-76 cells, PLXND1 binding peptide treatment resulted in a reduction of p-ERK, a cell growth marker, a reduction in N-Cadherin (**N-Cad**), an increase in E-Cadherin (**E-Cad**), and a reduction in Snail, which reflect a reduction in EMT shift (**Figure 5a,b**).[32,33] The observed reduction in cell growth and tumor migration markers suggests that PLXND1 may be a therapeutically effective target for inhibiting tumor growth and migration in SHH MB.

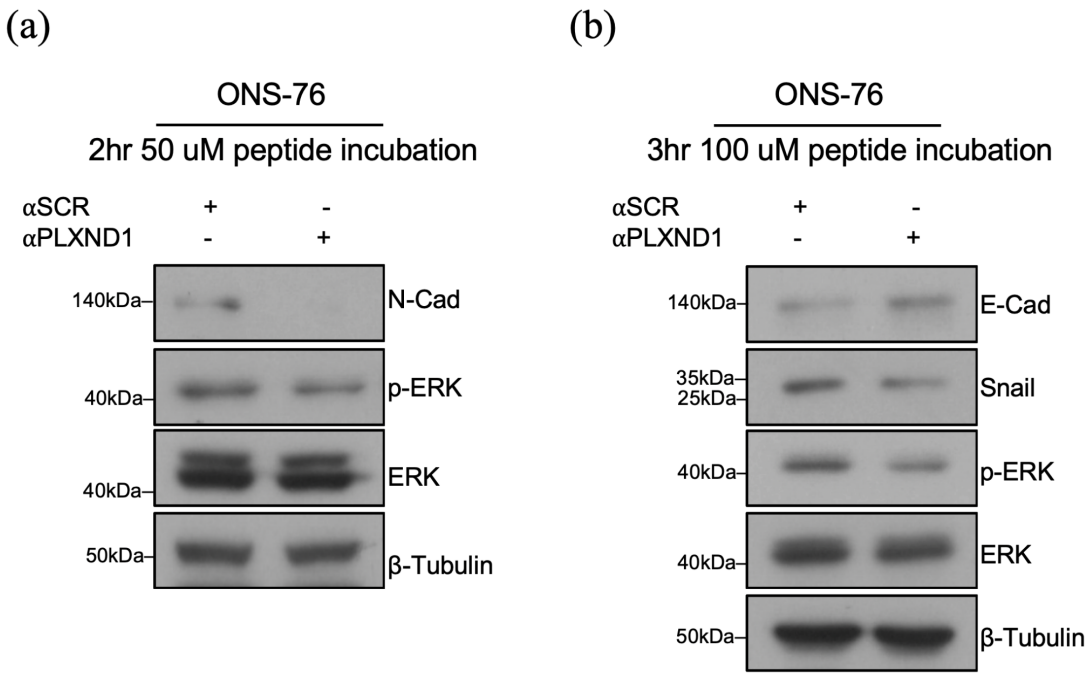

**Figure 5: PLXND1 binding peptide results in reduced cell growth and EMT markers**

**(A)** Western blotting in ONS-76 cells showing reduced N-Cad and p-ERK alongside total ERK and β-tubulin after a 2 hour, 50uM PLXND1 binding peptide incubation. **(B)** Western blotting in ONS-76 cells showing increased E-Cad and reduced Snail and p-ERK alongside total ERK and β-tubulin after a 3 hour, 100uM PLXND1 binding peptide incubation.

**SEMA3E and NRP1 colocalize with PLXND1**

To assess the cell surface localization of SEMA3E, NRP1, and PLXND1, immunofluorescence staining was performed in PZP and MBC cells. SEMA3E and PLXND1 merged images show colocalization of the two proteins. (**Figure 6a**). NRP1 and PLXND1 merged

images also show colocalization, leading us to hypothesize that SEMA3E and NRP1 are both binding to and signaling through PLXND1 (**Figure 6b**).

**Figure 6: SEMA3E and NRP1 colocalize with PLXND1.** (**A**) Immunofluorescent staining of SEMA3E (*green*) and PLXND1 (*red*) in MBC and PZP cells, and staining of DAPI for nuclei (*blue*). (**B**) Immunofluorescent staining of NRP1 (*green*) and PLXND1 (*red*) in MBC and PZP

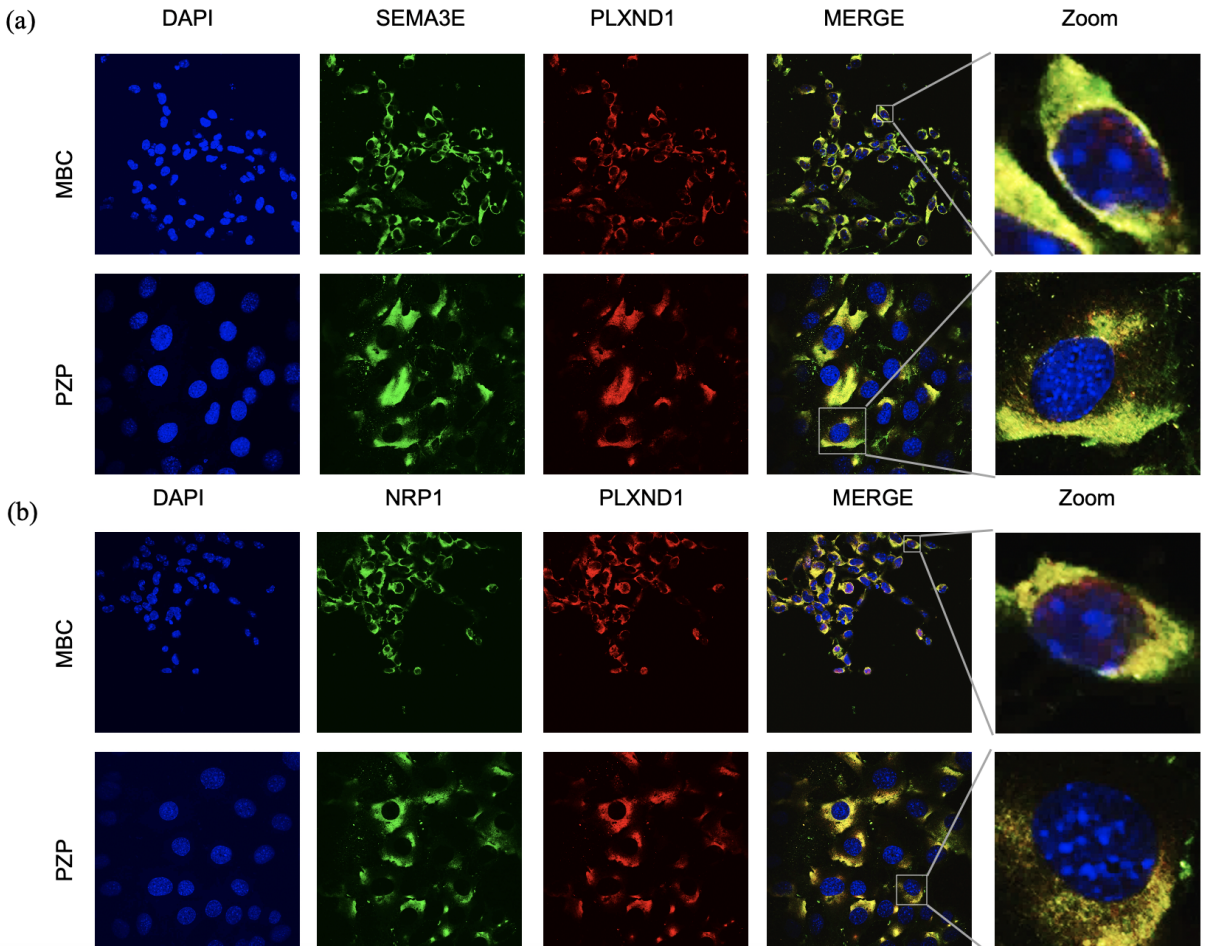


cells, and staining of DAPI for nuclei (*blue*).

**SEMA3E is elevated in SHH MB, glycosylated, and secreted**

To characterize SEMA3E protein expression profile in SHH MB, we performed Western Blotting on NeuroD2-SmoA1 green fluorescence protein (**GFP**) positive primary mouse MB cells.

As previously mentioned, activating mutations in Smoothened gene (**Smo**) that constitutively activate the Shh pathway is one characteristic of SHH MB.[34] The NeuroD2-SmoA1 GFP positive transgenic mice is a model of SHH MB that constitutively expresses Smo in CGNPs.[35] By six months of age, 94% of the mice develop cerebellar tumors, which express GFP that allows for easy identification of tumor and non-tumor tissues.[36]

We previously showed that PLXND1 protein levels are elevated in tumor tissue, leading us to explore SEMA3E expression in primary mouse MB tumors. We isolated both tumor and matched cerebellar tissue from our NeuroD1-SmoA1 GFP positive mice models and showed that SEMA3E protein levels are enriched in primary mouse SHH MB tumor tissue (**MB**) relative to matched non-tumor cerebellar tissue (**CB**) (**Figure 7a**). Since current research shows that SEMA3E may undergo cleavage, we performed immunoblotting to investigate the full and cleaved SEMA3E lengths in our models and to validate the bands we observed upon probing for SEMA3E in Western Blotting. Interestingly, we showed that full length SEMA3E is found at around 100 kDa, with two cleaved isoforms at around 60 kDa and 35 kDa in astrocyte, MBC, PZP, and ONS-76 SHH MB cell lines, indicative of SEMA3E cleavage in our models (**Figure 7b**). Contrary to the published full length protein size of 89 kDa for SEMA3E, we noticed that SEMA3E on our blots had been larger, at around 100 kDa.[37] Thus, we investigated whether the 100 kDa SEMA3E band was due to glycosylation by adding N-glycosidase F (**PNGase F**), a deglycosylation enzyme.[38] Following PNGase F treatment in PZP cells, we observed the published 89 kDa SEMA3E band, indicating that SEMA3E is glycosylated in our SHH MB models (**Figure 7c**). Understanding the glycosylation of SEMA3E in our models provides support for our proper Western Blotting identification of SEMA3E and may suggest glycosylation-dependent functions of the protein. Current literature suggests differing activity of secreted and membrane-bound

SEMA3E, leading us to investigate whether SEMA3E is secreted in our models.[39] Thus, we showed SEMA3E secretion into the tumor cell environment by concentrating FBS-free media of PZP and ONS-76 cell lines; we ran the concentrated media supernatant (**Sup.**) with whole cell lysate (**WCL**) and a blank negative control (**Figure 7d**). Our findings of enriched SEMA3E protein levels in MB tissue and presence of cleaved, glycosylated, and secreted SEMA3E in our models lead us to explore the functional roles of SEMA3E in promoting MB migration.

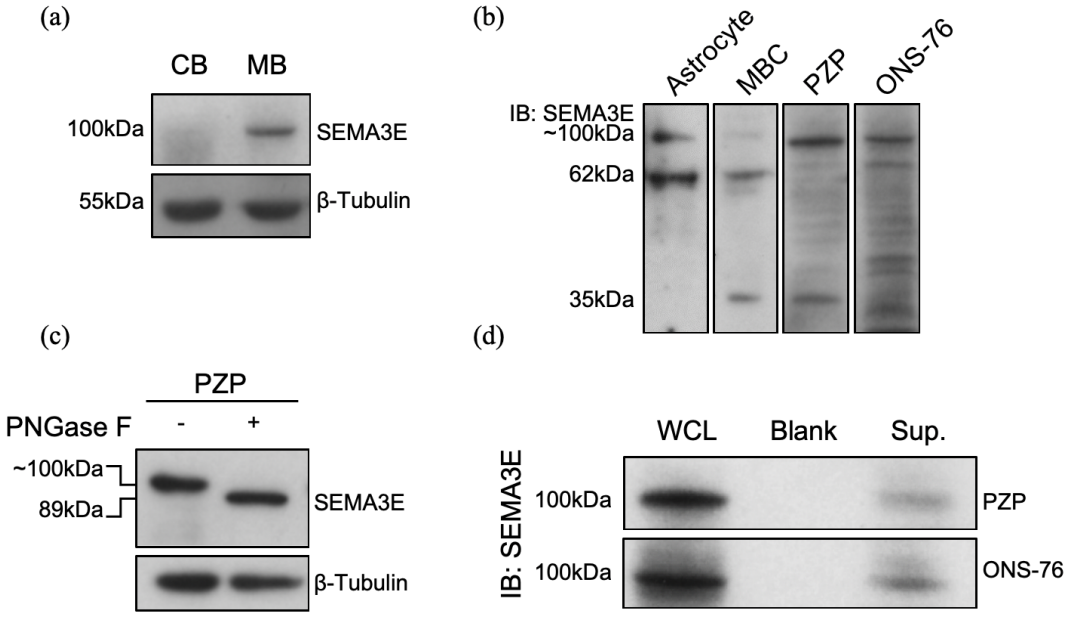

**Figure 7: SEMA3E is elevated in SHH MB, glycosylated, and secreted.** (**A**) Western blotting for SEMA3E in CB (cerebellar) and MB primary NeuroD1-SmoA1 GFP positive mouse samples. (**B**) Immunoblotting for full length and cleaved SEMA3E in astrocyte, MBC, PZP, and ONS-76 cells. (**C**) Western blotting for SEMA3E following PNGase F treatment. (**D**) Western blotting for SEMA3E in PZP and ONS-76 WCL and Sup.

**SEMA3E depletion results in reduced tumor cell migration but not proliferation**

To investigate the role of SEMA3E in tumor migration, we performed *in vitro* wound healing scratch assays using SEMA3E stable knockdown cells (shSEMA3E_34 and shSEMA3E_35) in both UW228 and ONS-76 cell lines (**Figure 8 a,c**). We observed a significant reduction in wound closure upon SEMA3E knockdown compared to the shSCR control at both time points (T24 and T48) and in both cell lines and SEMA3E knockdown constructs. At 24 hours post-scratch, wound closure in UW228 cells was reduced by an average of 28.90% and 33.41% in the shSEMA3E_34 and shSEMA3E_35 constructs, respectively (**Figure 8b**). At 48 hours post-scratch, wound closure in UW228 cells was reduced by an average of 46.29% and 49.16% in the shSEMA3E_34 and shSEMA3E_35 constructs, respectively (**Figure 8b**). In ONS-76 cells at 24 hours post-scratch, wound closure was reduced by an average of 19.55% and 20.42% in the shSEMA3E_34 and shSEMA3E_35 constructs respectively; by 48 hours post-scratch, would closure was reduced by an average of 29.11% and 29.79% in the shSEMA3E_34 and shSEMA3E_35 constructs respectively (**Figure 8d**). These significant reductions in wound closure upon SEMA3E knockdown suggest a role of SEMA3E in promoting cell migration in SHH MB.

In contrast, there was no overall difference in proliferation among the shSCR and shSEMA3E knockdown constructs. In both UW228 and ONS-76 cell lines, there was no significant difference in proliferation except in the ONS-76 shSEMA_35 construct, which showed an average 62.25% reduction in proliferation at four days after plating (**Figure 8f**).

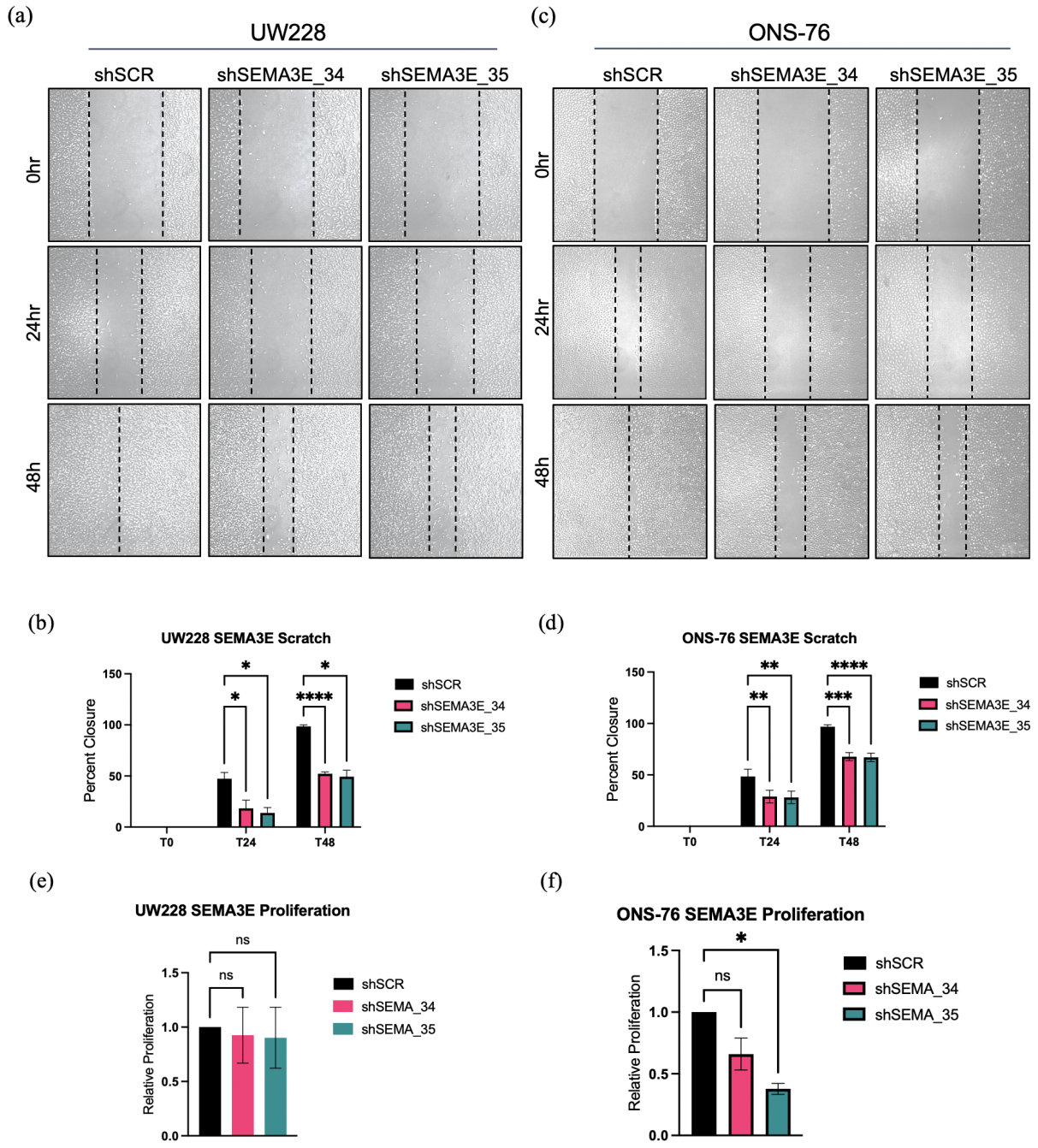


**Figure 8: SEMA3E depletion results in reduced tumor cell migration but not proliferation.**

**(A)** *In vitro* wound healing scratch assays in UW228 cell line with SEMA3E knockdown

(shSEMA3E_34 and shSEMA3E_35). (**B**) Wound closure analysis showing reduced percent closure in shSEMA3E_34 (T24, $p<0.05$; T48, $p<0.0001$) and shSEMA3E_35 (T24, $p<0.05$, T48, $p<0.05$). Two-way ANOVA comparing knockdown to control cell line, n=3. (**C**) *In vitro* wound healing scratch assays in ONS-76 cells with SEMA3E knockdown (shSEMA3E_34 and shSEMA3E_35). (**D**) Wound closure analysis showing reduced percent closure in shSCR vs shSEMA3E_34 (T24, $p=0.0042$; T48, $p<0.001$, n=3) and shSEMA3E_35 (T24, $p=0.003$, T48, $p<0.0001$, n=3). (**E**) Relative proliferation of SEMA3E depleted cells at four days post-plating in UW228 cell lines showing no significance. Two-way ANOVA comparing knockdown to control cell line, n=3. (**F**) Relative proliferation analysis of SEMA3E knockdown cells at four days post-plating in ONS-76 cell lines. shSCR vs shSEMA3E_34 ($p=0.0901$) and shSEMA3E_35 ($p=0.0189$). Two-way ANOVA comparing knockdown to control cell line, n=2.

**SEMA3E depletion results in inconsistent EMT shift**

EMT is a hallmark of tumor metastasis, invasion, and chemotherapy resistance.[40] To better understand the mechanisms by which SEMA3E may drive tumor metastasis, we sought to characterize EMT shifts upon SEMA3E knockdown. Overall, the trends in EMT marker shifts were inconsistent among SEMA3E knockdown constructs and UW228 and ONS-76 cell lines (**Figure 9a, b**). The only proteins that showed a consistent decrease in EMT among both knockdown constructs were claudin in UW228 cells and N-cadherin in ONS-76 cells. However, the majority of measured EMT markers showed inconsistent trends, which could indicate that SEMA3E does not play a significant role in SHH MB EMT shifts or that a shRNA knockdown did not sufficiently deplete SEMA3E secretion into the supernatant.

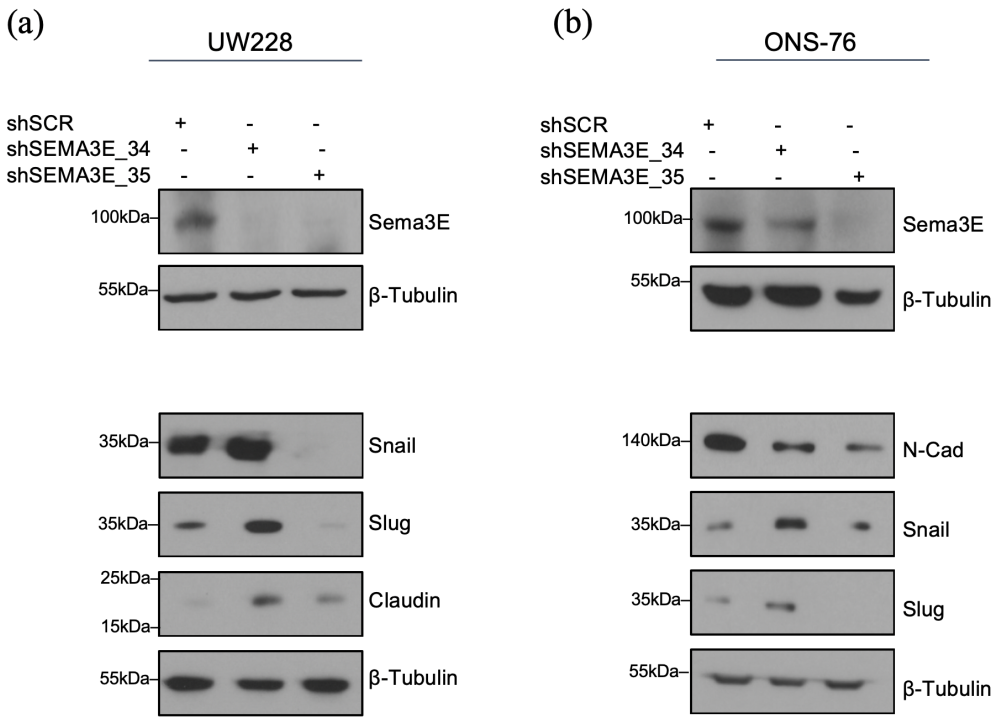


**Figure 9: SEMA3E depletion results in inconsistent EMT shift. (A)** Western blotting in UW228 cell line showing SEMA3E knockdown and select EMT marker changes upon SEMA3E knockdown. **(B)** Western blotting in ONS-76 cell line showing SEMA3E knockdown and select EMT marker changes upon SEMA3E knockdown.

**NRP1 depletion results in reduced tumor migration and EMT shift but not proliferation**

So far we have shown SEMA3E, the canonical binding ligand to PLXND1, to be involved in tumor cell migration and proliferation, with inconsistencies in driving EMT shift. We next investigated the functional importance of NRP1, the canonical binding partner to PLXND1, in promoting tumor migration. To investigate tumor cell migration, we performed *in vitro* wound-healing scratch assays on stable shRNA NRP1 knockdown cell lines shNRP1_17 and shNRP1_27

in ONS-76 cells (**Figure 10a**). We found a significant reduction in wound closure among both NRP1 knockdown constructs, shNRP1_17 and shNRP1_27, compared to shSCR at 24 hours ($p=0.0180$ and $p=0.0258$, respectively) and 48 hours ($p=0.0064$ and $p=0.0045$, respectively) post-scratch (**Figure 10b**). Consistent with current literature, our data suggests NRP1 may be involved in promoting tumor migration.[41] To further characterize the role NRP1 has in tumor invasion, we performed Western Blotting on ONS-76 shNRP1 cells to probe for EMT markers. Both NRP1 depleted samples showed a robust and consistent decrease in EMT shift, indicating the protein's involvement in promoting tumor expansion (**Figure 10c**). Since NRP1 is a co-receptor for PLXND1 and our PLXND1 depleted cells showed reduced tumor proliferation, we also investigated whether NRP1 may drive tumor proliferation. Surprisingly, both shNRP1_17 and shNRP1_27 cells showed no proliferative difference compared to shSCR control ($p=0.3183$ and $p=0.9227$, respectively) (**Figure 10d**). These data suggest NRP1 may promote tumor migration and expansion but may not have a strong effect on proliferation in SHH NB.

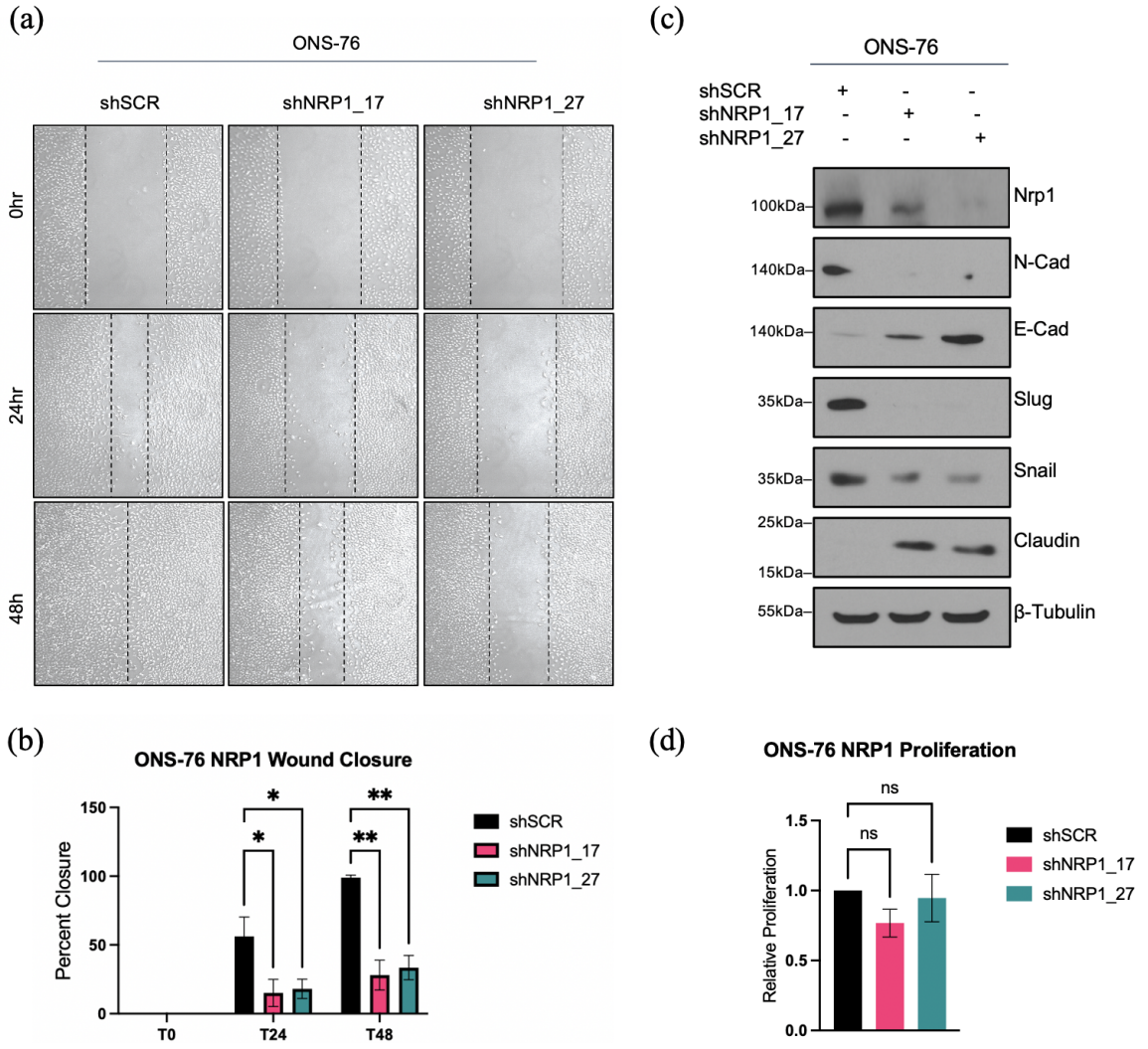


**Figure 10: NRP1 depletion results in reduced tumor migration and EMT shift but not proliferation**

**(A)** *In vitro* wound healing scratch assays in ONS-76 cell line with NRP1 knockdown (shNRP1_17 and shNRP1_27). **(B)** Wound closure analysis showing reduced percent closure in shNRP1_17 (T24, p=0.0180; T48, p=0.0064) and shNRP1_27 (T24, p=0.0258, T48, p=0.0045). Two-way ANOVA comparing knockdown to control cell line, n=3. **(C)** Western blotting in ONS-76 cell lines showing NRP1 knockdown in shNRP1_17 and shNRP1_27 cells and reduced EMT shift in NRP1 depleted cells.

## Discussion:

We extend our previous findings of YB-1 as a driver of tumorigenesis; in this study, we have elucidated PLXND1 as a novel post-transcriptional target of YB-1[7]. Specifically, we show that YB-1 positively modulates PLXND1 mRNA translation in SHH MB and thus propose a novel regulatory mechanism by which YB-1 promotes tumor cell migration through PLXND1. SEMA3E is a well-established binding partner to PLXND1, and NRP1 has been published as a PLXND1 co-receptor.[42] In our study, we showed cell surface colocalization of SEMA3E and NRP1 to PLXND1 in our SHH MB models. To better understand the mechanisms driving PLXND1-mediated tumor migration, we also further characterized SEMA3E expression in SHH MB, showing that it is both cleaved and glycosylated.

We investigated the functional significance of PLXND1, SEMA3E, and NRP1 in promoting tumor cell migration. Our findings were consistent with previous publications on human carcinomas, ovarian cancer, and lung cancer, which demonstrated reduced tumor cell migratory ability upon depletion of PLXND1, SEMA3E, and NRP1.[22,25,43] We showed that PLXND1 promotes tumor cell migration and growth in SHH MB–silencing PLXND1 expression resulted in a reduction of tumor migration and proliferation. While our data in ONS-76 and PZP cell lines show consistent acquisition of mesenchymal characteristics and loss of epithelial markers upon PLXND1 knockdown, these EMT trends were not consistent upon SEMA3E knockdown. The discrepancy between our findings and published literature showing SEMA3E facilitation of EMT in other cancer models may be explained through differences in SEMA3E functions between cancer types. Alternative explanations may be attributed to the continuous secretion and/or the incomplete knockdown of SEMA3E, thereby driving tumor migration and proliferation.

Additionally, there is evidence that SEMA3E promotes EMT through nuclear localization of Snail.[44] Thus, performing nuclear extraction to investigate Snail expression may produce more consistent results with published literature. We also recapitulated findings in SHH MB mouse models showing the requirement of NRP1 in promoting tumor migration. Previously, another group showed that NRP1 blockade resulted in MB regression, decreased metastasis, and longer mice survival, and thereby implicated NRP1 as a potential therapeutic target in SHH MB.[45] We extended these findings by showing consistent reduction in EMT shift upon NRP1 knockdown. Although PLXND1, SEMA3E, and NRP1 promote tumor cell migration, we found that PLXND1 and NRP1 depleted tumor cells exhibited stronger reductions in wound closure rate and EMT shifts than SEMA3E knockdown cells.

Our findings suggest that SEMA3E may not be the primary driver of tumor migration in SHH MB, as SEMA3E knockdown resulted in the weakest antitumor phenotypes compared to PLXND1 and NRP1 knockdown. One possible explanation for the weak phenotype is the complex nature of semaphorin signaling. Semaphorins can bind in cis (within the same cell) and in trans, and class 3 (A–H) and 4 (A–G) semaphorins can all bind to PLXND1.[46] Cis and trans binding alters inhibitory and stimulatory interactions with plexins, such that semaphorin cis binding prevents its trans interactions with plexins while activating its cis interactions.[9] Given our *in vitro* experiments, the MB cells are likely experiencing both in cis and in trans activation due to the presence of secreted SEMA3E in the media. The complexity and non-specific binding of semaphorins to PLXND1 may explain the weak and inconsistent phenotype of SEMA3E knockdown, making it difficult to distinguish the main driver(s) of PLXND1-mediated SHH MB migration and invasion. We have also demonstrated that astrocytes, in addition to SHH MB cells, secrete SEMA3E into the supernatant. SEMA3E secretion complicates *in vivo* studies, as other

neurons may compensate for the SEMA3E depletion by secreting the protein into the cellular environment. Therefore, complete SEMA3E knockout would be essential to investigate the specific role of SEMA3E in SHH MB migration and invasion *in vivo*.

Our findings on the role of PLXND1 in promoting SHH MB migration suggest that PLXND1 may be a relevant therapeutic target for SHH MB treatment–a claim that select published literature has also made.[25,47,48] We showed *in vitro* that depleting PLXND1 reduced tumor growth, migration, and invasive properties. Another group developed a PLXND1 binding peptide and showed a reduction in tumor volume in NSG mice with pancreatic ductal adenocarcinoma when treated with the peptide.[12] After synthesizing this peptide, we showed a reduction in cell growth and EMT shift in ONS-76 cells upon peptide treatment. Given the prevalence of PLXND1 overexpression in most carcinomas and our PLXND1-binding peptide data, therapeutic targeting of PLXND1 may be a promising potential treatment for SHH MB.[48]

One main limitation of the current work is our lack of *in vivo* models. As a future direction, we plan to investigate tumor migration of shPLXND1 spheres on wild-type mice cerebellar tissue (neurosphere on slice culture). The neurosphere on slice culture experiment will better reflect *in vivo* conditions than cell culture alone. If the shPLXND1 spheres show reduced migration, another potential next step is to conduct NSG pup injections with shPLXND1 GFP positive cells and compare tumor progression with and without the PLXND1 binding peptide. Since the PLXND1 binding peptide disrupts PLXND1 binding to TGFβ, we can potentially interrogate the PLXND1/TGFβ signaling in SHH MB by conducting a CO-IP on cells treated with the peptide and probe for the presence of TGFβ bound to PLXND1. Lastly, to better understand the requirement of SEMA3E and NRP1 in PLXND1-mediated migration, we plan to conduct a PLXND1 CO-IP to probe for both SEMA3E and NRP1.

## References:


1. Millard NE, De Braganca KC. Medulloblastoma. *J Child Neurol*. 2016;31(12):1341-1353.

2. Juraschka K, Taylor MD. Medulloblastoma in the age of molecular subgroups: a review. *J Neurosurg Pediatr*. 2019;24(4):353-363.

3. Tamayo-Orrego L, Charron F. Recent advances in SHH medulloblastoma progression: tumor suppressor mechanisms and the tumor microenvironment. *F1000Res*. 2019;8. doi:10.12688/f1000research.20013.1

4. Skoda AM, Simovic D, Karin V, Kardum V, Vranic S, Serman L. The role of the Hedgehog signaling pathway in cancer: A comprehensive review. *Bosn J Basic Med Sci*. 2018;18(1):8-20.

5. Lazow MA, Palmer JD, Fouladi M, Salloum R. Medulloblastoma in the Modern Era: Review of Contemporary Trials, Molecular Advances, and Updates in Management. *Neurotherapeutics*. 2022;19(6):1733-1751.

6. Dey A, Robitaille M, Remke M, et al. YB-1 is elevated in medulloblastoma and drives proliferation in Sonic hedgehog-dependent cerebellar granule neuron progenitor cells and medulloblastoma cells. *Oncogene*. 2016;35(32):4256-4268.

7. Sangermano F, Delicato A, Calabrò V. Y box binding protein 1 (YB-1) oncoprotein at the hub of DNA proliferation, damage and cancer progression. *Biochimie*. 2020;179:205-216.

8. Lyabin DN, Eliseeva IA, Ovchinnikov LP. YB-1 protein: functions and regulation. *Wiley Interdiscip Rev RNA*. 2014;5(1):95-110.

9. Gay CM, Zygmunt T, Torres-Vázquez J. Diverse functions for the semaphorin receptor PlexinD1 in development and disease. *Dev Biol*. 2011;349(1):1-19.

10. Tamagnone L, Artigiani S, Chen H, et al. Plexins are a large family of receptors for transmembrane, secreted, and GPI-anchored semaphorins in vertebrates. *Cell*. 1999;99(1):71-80.

11. Limoni G, Niquille M. Semaphorins and Plexins in central nervous system patterning: the key to it all? *Curr Opin Neurobiol*. 2021;66:224-232.

12. Vivekanandhan S, Madamsetty VS, Angom RS, et al. Role of PLEXIND1/TGFβ Signaling Axis in Pancreatic Ductal Adenocarcinoma Progression Correlates with the Mutational Status of KRAS. *Cancers* . 2021;13(16). doi:10.3390/cancers13164048

13. Chauvet S, Cohen S, Yoshida Y, et al. Gating of Sema3E/PlexinD1 signaling by neuropilin-1 switches axonal repulsion to attraction during brain development. *Neuron*. 2007;56(5):807-822.

14. Shen M, Chen Y, Tang W, et al. Semaphorin 3E promote Schwann cell proliferation and migration. *Exp Cell Res*. 2022;412(2):113019.

15. Liu ZZ, Guo J, Lu Y, et al. Sema3E is required for migration of cranial neural crest cells in zebrafish: Implications for the pathogenesis of CHARGE syndrome. *Int J Exp Pathol*. 2019;100(4):234-243.

16. Velona T, Altounian M, Roque M, et al. PlexinD1 and Sema3E determine laminar positioning of heterotopically projecting callosal neurons. *Mol Cell Neurosci*. 2019;100:103397.

17. Bribián A, Nocentini S, Llorens F, et al. Sema3E/PlexinD1 regulates the migration of hem-derived Cajal-Retzius cells in developing cerebral cortex. *Nat Commun*. 2014;5:4265.

18. Sawada M, Ohno N, Kawaguchi M, et al. PlexinD1 signaling controls morphological changes and migration termination in newborn neurons. *EMBO J*. 2018;37(4). doi:10.15252/embj.201797404

19. Van Battum E, Heitz-Marchaland C, Zagar Y, Fouquet S, Kuner R, Chédotal A. Plexin-B2 controls the timing of differentiation and the motility of cerebellar granule neurons. *Elife*. 2021;10. doi:10.7554/eLife.60554

20. Bagri A, Tessier-Lavigne M. Neuropilins as Semaphorin receptors: in vivo functions in neuronal cell migration and axon guidance. *Adv Exp Med Biol*. 2002;515:13-31.

21. Vivekanadhan S, Mukhopadhyay D. Divergent roles of Plexin D1 in cancer. *Biochim Biophys Acta Rev Cancer*. 2019;1872(1):103-110.

22. Tseng CH, Murray KD, Jou MF, Hsu SM, Cheng HJ, Huang PH. Sema3E/plexin-D1 mediated epithelial-to-mesenchymal transition in ovarian endometrioid cancer. *PLoS One*. 2011;6(4):e19396.

23. Maejima R, Tamai K, Shiroki T, et al. Enhanced expression of semaphorin 3E is involved in the gastric cancer development. *Int J Oncol*. 2016;49(3):887-894.

24. Jurcak NR, Rucki AA, Muth S, et al. Axon Guidance Molecules Promote Perineural Invasion and Metastasis of Orthotopic Pancreatic Tumors in Mice. *Gastroenterology*. 2019;157(3):838-850.e6.

25. Casazza A, Finisguerra V, Capparuccia L, et al. Sema3E-Plexin D1 signaling drives human cancer cell invasiveness and metastatic spreading in mice. *J Clin Invest*. 2010;120(8):2684-2698.

26. Hagihara K, Haraguchi N, Nishimura J, et al. PLXND1/SEMA3E Promotes Epithelial-Mesenchymal Transition Partly via the PI3K/AKT-Signaling Pathway and Induces Heterogenity in Colorectal Cancer. *Ann Surg Oncol*. 2022;29(12):7435-7445.

27. Roche J. The Epithelial-to-Mesenchymal Transition in Cancer. *Cancers* . 2018;10(2).

doi:10.3390/cancers10020052

28. Luchino J, Hocine M, Amoureux MC, et al. Semaphorin 3E suppresses tumor cell death triggered by the plexin D1 dependence receptor in metastatic breast cancers. *Cancer Cell*. 2013;24(5):673-685.

29. Berman DM, Karhadkar SS, Hallahan AR, et al. Medulloblastoma growth inhibition by hedgehog pathway blockade. *Science*. 2002;297(5586):1559-1561.

30. Guo N, Peng Z. MG132, a proteasome inhibitor, induces apoptosis in tumor cells. *Asia Pac J Clin Oncol*. 2013;9(1):6-11.

31. Sobell HM. Actinomycin and DNA transcription. *Proc Natl Acad Sci U S A*. 1985;82(16):5328-5331.

32. Mebratu Y, Tesfaigzi Y. How ERK1/2 activation controls cell proliferation and cell death: Is subcellular localization the answer? *Cell Cycle*. 2009;8(8):1168-1175.

33. Loh CY, Chai JY, Tang TF, et al. The E-Cadherin and N-Cadherin Switch in Epithelial-to-Mesenchymal Transition: Signaling, Therapeutic Implications, and Challenges. *Cells*. 2019;8(10). doi:10.3390/cells8101118

34. Dey J, Ditzler S, Knoblaugh SE, et al. A distinct Smoothened mutation causes severe cerebellar developmental defects and medulloblastoma in a novel transgenic mouse model. *Mol Cell Biol*. 2012;32(20):4104-4115.

35. Hallahan AR, Pritchard JI, Hansen S, et al. The SmoA1 mouse model reveals that notch signaling is critical for the growth and survival of sonic hedgehog-induced medulloblastomas. *Cancer Res*. 2004;64(21):7794-7800.

36. Hatton BA, Villavicencio EH, Tsuchiya KD, et al. The Smo/Smo model: hedgehog-induced medulloblastoma with 90% incidence and leptomeningeal spread. *Cancer Res*. 2008;68(6):1768-1776.

37. Wanschel A, Seibert T, Hewing B, et al. Neuroimmune guidance cue Semaphorin 3E is expressed in atherosclerotic plaques and regulates macrophage retention. *Arterioscler Thromb Vasc Biol*. 2013;33(5):886-893.

38. Tarentino AL, Gómez CM, Plummer TH Jr. Deglycosylation of asparagine-linked glycans by peptide:N-glycosidase F. *Biochemistry*. 1985;24(17):4665-4671.

39. Alamri A, Soussi Gounni A, Kung SKP. View Point: Semaphorin-3E: An Emerging Modulator of Natural Killer Cell Functions? *Int J Mol Sci*. 2017;18(11). doi:10.3390/ijms18112337

40. Pastushenko I, Blanpain C. EMT Transition States during Tumor Progression and Metastasis. *Trends Cell Biol*. 2019;29(3):212-226.

41. Douyère M, Chastagner P, Boura C. Neuropilin-1: A Key Protein to Consider in the Progression of Pediatric Brain Tumors. *Front Oncol*. 2021;11:665634.

42. Oh WJ, Gu C. The role and mechanism-of-action of Sema3E and Plexin-D1 in vascular and neural development. *Semin Cell Dev Biol*. 2013;24(3):156-162.

43. Ding Z, Du W, Lei Z, et al. Neuropilin 1 modulates TGF-β1-induced epithelial-mesenchymal transition in non-small cell lung cancer. *Int J Oncol*. 2020;56(2):531-543.

44. Campo L, Zhang C, Breuer EK. EMT-Inducing Molecular Factors in Gynecological Cancers. *Biomed Res Int*. 2015;2015:420891.

45. Snuderl M, Batista A, Kirkpatrick ND, et al. Targeting placental growth factor/neuropilin 1 pathway inhibits growth and spread of medulloblastoma. *Cell*. 2013;152(5):1065-1076.

46. Alto LT, Terman JR. Semaphorins and their Signaling Mechanisms. *Methods Mol Biol*. 2017;1493:1-25.

47. Rehman M, Gurrapu S, Cagnoni G, Capparuccia L, Tamagnone L. PlexinD1 Is a Novel Transcriptional Target and Effector of Notch Signaling in Cancer Cells. *PLoS One*. 2016;11(10):e0164660.

48. Roodink I, Verrijp K, Raats J, Leenders WPJ. Plexin D1 is ubiquitously expressed on tumor vessels and tumor cells in solid malignancies. *BMC Cancer*. 2009;9:297.